Analytical Methods

PAPER

View Article Online
View Journal | View Issue

Cite this: *Anal. Methods*, 2015, **7**, 7474

A turn-on upconversion fluorescence resonance energy transfer biosensor for ultrasensitive endonuclease detection†

Li-Jiao Huang, Xue Tian, Jin-Tao Yi, Ru-Qin Yu and Xia Chu*

Received 6th May 2015
Accepted 27th June 2015

DOI: 10.1039/c5ay01169h

www.rsc.org/methods

A facile one-step approach was proposed to make hydrophilic and DNA-functionalizable upconversion nanoparticles through ligand exchange at the liquid–liquid interface, and an ultrasensitive and selective biosensor for nuclease assay and its inhibitors assay based on FRET from the DNA-functionalizable UCNPs to graphene oxide was designed. A high sensitivity exhibited with a detectable minimum concentration of 1×10^{-4} units per mL S1 nuclease, which was more sensitive than the developed approaches.

1 Introduction

Fluorescence resonance energy transfer (FRET) is a classic homogeneous assay technique based on the strength of transfer donors' nonradiative energy to acceptors, which are close to each other (normally 1–10 nm), *via* dipole–dipole interactions. When coupled with the high sensitivity of fluorescence, FRET has been recognized as a magnificent sensitive method and has been widely used in bioassays. Currently, various fluorescence resonance energy transfers (FRETs) between emerging nanomaterials and biomolecular recognition units have shown great potential for the development of novel clinic diagnostic techniques.[1,2] However, traditional downconversion nanomaterials and organic dyes commonly used as donors in the FRET process are usually excited using ultraviolet or blue light, which tends to give rise to strong background fluorescence from the endogenous chromophores in biological or environmental samples, thus limiting their applications in complex biological samples.[3]

Lanthanide-doped upconversion nanoparticles (UCNPs), which are capable of emitting strong visible fluorescence under the excitation of near-infrared (NIR) light (typically *ca.* 980 nm), have attracted considerable attention. These UCNPs have shown significant advantages over the traditional downconversion nanomaterials due to their superior optical and chemical features, such as improved quantum yield, minimal photobleaching, reinforced light penetration depth in tissue, and low toxicity.[4] More importantly, under the excitation of NIR light, the effect of autofluorescence from complex samples and scattering light becomes negligible. These merits make UCNPs an ideal candidate as a fluorescent probe. Up to now, a lot of research has reported the detection of ions,[5] small molecules,[6,7] proteins,[8,9] and nucleic acids[10,11] based on UCNP fluorescent probes.

To develop UCNP-based biosensors, a major challenge is to make water-dispersible, biocompatible and functionalizable UCNPs, because they are normally prepared in organic solvents and capped with hydrophobic ligands.[12] Many approaches such as one-step solvothermal synthesis,[13,14] silica coating[15] and phospholipid coating[16] have been developed to solve this problem. Our group has also prepared phospholipid-modified UCNPs for the detection of phospholipase D[17] and human immunodeficiency virus antibody.[18] Recently, Lu's group has reported an approach to prepare DNA-functionalized UCNPs based on a ligand exchange process,[19] which not only converts hydrophobic UCNPs into water-dispersible and biocompatible ones, but also avoids the extra steps of bioconjugations using cross-linkers.

Here we developed water-dispersible and DNA-functionalized UCNPs based on a facile one-step ligand exchange approach, and designed a biosensor based on FRET from the DNA-functionalizable UCNPs to graphene oxide (GO), a highly efficient energy transfer acceptor.[20,21] To demonstrate the utility of this strategy, we chose an endonuclease assay as the model system. Endonucleases play a vital role in a variety of biological processes involving replication, recombination, DNA repair, molecular cloning, genotyping, and mapping.[22,23] Moreover, the assay of endonuclease activity and inhibition is of high importance in the fields ranging from biotechnology to pharmacology. Due to their intrinsic biological importance and use in a wide range of applications, development of sensitive methods for nuclease activity assay is essential in the fields of molecular biology, biomedicine, nanoscience, and biosensing.

State Key Laboratory for Chemo/biosensing and Chemometrics, College of Chemistry and Chemical Engineering, Hunan University, Changsha, 410082, PR China. E-mail: xiachu@hnu.edu.cn; rqyu@hnu.edu.cn; Fax: +86 731 88821916; Tel: +86 731 88821916

† Electronic supplementary information (ESI) available: Experimental details and additional figures. See DOI: 10.1039/c5ay01169h

2 Experimental

2.1 Reagents and apparatus

Rare-earth chlorides used in this work including $YCl_3 \cdot 6H_2O$, $YbCl_3 \cdot 6H_2O$ $Tm(CH_3COO)_3 \cdot xH_2O$, NH_4F, NaOH, oleic acid, 1-octadecene and thrombin were all purchased from Sigma-Aldrich (U.S.A.). Cyclohexane and ethanol were of analytical grade and were purchased from Sinopharm Chemical Reagent Co., Ltd (Shanghai, China). ATP and the purified DNA oligonucleotide (5′ phosphate-CGCAAAAAAGAGAGTAA-3′) used in this work were obtained from Shanghai Sangon Biological Science & Technology Company (Shanghai, China). BSA and S1 nuclease (100 units μL^{-1}) were obtained from Thermo Fisher Scientific Inc. The S1 nuclease buffer (20 mM NaAc, 150 mM NaCl, and 1 mM $ZnSO_4$, pH 4.5) was used to dilute the S1 nuclease and enzymatic digestion reaction. Exonuclease III (*E. coli*) and Bst polymerase were purchased from New England Biolabs (Ipswich, MA, USA). All of the solutions were prepared using ultrapure water (>18.25 MΩ) produced by a Millipore Milli-Q water purification system (Billerica, MA, USA).

The upconversion fluorescence measurements were carried out on a FluoroMax-4 Spectrofluorometer (HORIBA Jobin Yvon, Inc., NJ, USA) equipped with an external 980 nm diode CW laser (Changchun New Industries Optoelectronics Tech. Co., Ltd.) as the excitation source instead of the internal excitation source. The fluorescence emission spectra were collected from 300 nm to 550 nm at room temperature with a 980 nm excitation wavelength. The morphologies of the nanoparticles were observed using a JEOL JEM-2100 transmission electron microscope (TEM). Dilute colloid solutions of the OA-coated UCNPs dispersed in cyclohexane and DNA-modified UCNPs dispersed in water were drop-cast on thin, carbon formvar-coated copper grids. The X-ray diffraction (XRD) pattern of the OA-coated UCNPs was obtained using a Rigaku D/Max-Ra X-ray diffractometer using a Cu target radiation source ($\lambda = 0.14428$ nm). The hydrodynamic size distribution and zeta potential distribution of the DNA-modified UCNPs were determined using a Malvern Zetasizer (Nano-ZS, USA). Fourier-transform infrared (FT-IR) spectrum analysis was performed with a Nicolet 4700 Fourier transform infrared spectrophotometer (Thermo Electron Co., USA) by using the KBr method. X-ray photoelectron spectroscopy (XPS) spectra were obtained using a 180° double focal hemisphere analyzer-128 channel detector, using an unmonochromated Al Kα X-ray source (Thermo Fisher Scientific, UK). The UV-vis absorption spectrum was recorded on a UV-2450 UV-vis spectrometer (Shimadzu, Japan).

2.2 Synthesis of the oleic acid-coated $NaYF_4$:Yb,Tm@$NaYF_4$ UCNPs

Water-insoluble oleic acid-coated $NaYF_4$:Yb,Tm@$NaYF_4$ nanoparticles (OA-UCNPs) were synthesized according to the method described in the literature with slight modification.[24] $NaYF_4$:Yb,Tm core nanoparticles were first synthesized. Briefly, $YCl_3 \cdot 6H_2O$ (0.695 mmol), $YbCl_3 \cdot 6H_2O$ (0.30 mmol), and $TmCl_3 \cdot 6H_2O$ (0.005 mmol) (1 mmol, Y : Yb : Tm = 69.5% : 30% : 0.5%) were added to a 50 mL three-necked flask containing oleic acid (OA) (8 mL) and 1-octadecene (15 mL). The reaction mixture was heated to 100 °C under vacuum with stirring for 30 min to remove residual water and oxygen and then heated to 160 °C for another 30 min to form a homogeneous solution and then cooled down to room temperature. Then, 10 mL of a methanol solution containing NaOH (2.5 mmol) and NH_4F (4 mmol) was added slowly and the resultant solution was stirred for an additional 30 min at 50 °C. The reaction mixture was heated to 70 °C under vacuum to remove methanol and then was rapidly heated to 300 °C under stirring and kept at this temperature for 1 h under Ar protection and then cooled down to room temperature. The resulting nanoparticles were precipitated by the addition of ethanol, collected using centrifugation at 8000 rpm for 5 min, washed several times with ethanol and the resulting $NaYF_4$:Yb,Tm core nanoparticles were obtained. Synthesis of the $NaYF_4$:Yb,Tm@$NaYF_4$ core–shell nanoparticles was performed in a similar manner except varying the amount of Y^{3+} ions. $YCl_3 \cdot 6H_2O$ (0.4 mmol) was added to a 50 mL three-necked flask containing oleic acid (OA) (8 mL) and 1-octadecene (15 mL). The reaction mixture was heated to 100 °C under vacuum with stirring for 30 min to remove residual water and oxygen and then heated to 160 °C for another 30 min to form a homogeneous solution, then cooled down to room temperature. $NaYF_4$:Yb,Tm core nanoparticles in 2 mL of cyclohexane were added along with a 5 mL methanol solution of NH_4F (2.5 mmol) and NaOH (4 mmol). The resulting mixture was stirred at 50 °C for 30 min, and then the reaction temperature was increased to 80 °C to remove the methanol and cyclohexane. Then the solution was heated to 300 °C under an argon flow for 1 h and cooled down to room temperature. The resulting nanoparticles were precipitated by adding ethanol, collected using centrifugation, washed with ethanol several times, and dried under vacuum for further experiments.

2.3 Preparation of the DNA-modified UCNPs

The preparation of the DNA-modified UCNPs was carried out according to the previously reported paper.[19] A water solution (2 mL) containing 0.6 nmol DNA oligonucleotides was slowly added to the OA-coated UCNPs (1 mg) in 1 mL of cyclohexane, and the solution was vigorously stirred for 18 h. Afterward, the UCNPs were clearly transferred into the water layer from the cyclohexane layer through the ligand exchange at the liquid–liquid interface. The water solution was then transferred to a microtube. After vigorous sonication, excess DNA was removed from the UCNPs using centrifugation at 18 000 rpm for 16 min and the UCNPs were washed several times with ultrapure water. The obtained DNA-modified UCNPs were finally suspended in 0.8 mL of ultrapure water and stored at 4 °C for further experiments. The concentration of the DNA-modified UCNPs was calculated as ~1 mg mL^{-1}.

2.4 Preparation of graphene oxide (GO)

GO was prepared according to the method described in our previous work with some modification.[25] It was prepared by a modified Hummers method using graphite powder as a starting material, the GO suspension (~2 mg mL^{-1}) was sonicated in an

ice-bath using a probe-type sonicator under a power of 40 W for 4 h (work 2 s, rest 4 s). The resulting suspension was centrifuged at 12 000 rpm for 30 min, and then the sediments were discarded.

2.5 Assay of S1 nuclease activity and inhibition

For measurements of S1 nuclease activity, a 20 μL aliquot of reagent solution containing DNA-functionalized UCNPs (50 μg mL^{-1} of final concentration) and S1 nuclease of various concentrations was used to perform the enzymatic digestion reaction. The mixture was first incubated at 37 °C for 20 minutes, then GO (final concentration of 80 μg mL^{-1}) and ultrapure water were added to the mixture and further incubated at 37 °C for 60 min. The upconversion fluorescence spectra of the final mixture were measured using a FluoroMax-4 Spectrofluorometer (HORIBA Jobin Yvon, Inc., NJ, USA) equipped with an external 980 nm diode CW laser (Changchun New Industries Optoelectronics Tech. Co., Ltd) as the excitation source instead of the internal excitation source.

For the inhibition experiments, the inhibitor ATP of various concentrations was first introduced into the solution containing DNA-functionalized UCNPs, and then S1 nuclease was added. All other procedures were the same as the aforementioned assay of S1 nuclease activity.

3 Results and discussion

3.1 Design of the strategy

The principle of the upconversion FRET-based biosensor is shown in Scheme 1. The hydrophobic OA-coated UCNPs were first converted into water-dispersible DNA-functionalized UCNPs by using 5′-end phosphate-modified DNA oligonucleotides through the interaction between the negatively charged phosphates of the DNA with surface lanthanide ions. When adding GO, DNA-functionalized UCNPs could adsorb on the surface of the GO *via* π–π stacking interactions and hydrophobic interactions. The upconversion fluorescence could be completely quenched through the energy-transfer or electron-transfer processes. In contrast, if S1 nuclease was introduced into the system, DNA was cleaved into mono- or short-oligonucleotide fragments. Therefore the π–π stacking and hydrophobic interactions would be weakened, which kept the UCNPs far away from the GO surface, resulting in the decrease in quenching efficiency and the recovery of upconversion fluorescence.

3.2 Characterization of the UCNPs

Highly efficient upconverting $NaYF_4$:Yb,Tm@$NaYF_4$ core–shell nanoparticles were synthesized using oleic acid (OA) as the stabilizing agent. The size and morphology of the OA-capped UCNPs were characterized using transmission electron microscopy (TEM). The TEM image shows that these nanocrystals display a uniform hexagonal plate-like morphology with a mean size of approximately 58 nm (Fig. 1A). The X-ray diffraction (XRD) analysis (Fig. 1C) indicated that the peak positions and intensities of the nanocrystals agreed well with the calculated values of the pure hexagonal-phase nanocrystals (JCPDS no. 28-1192).

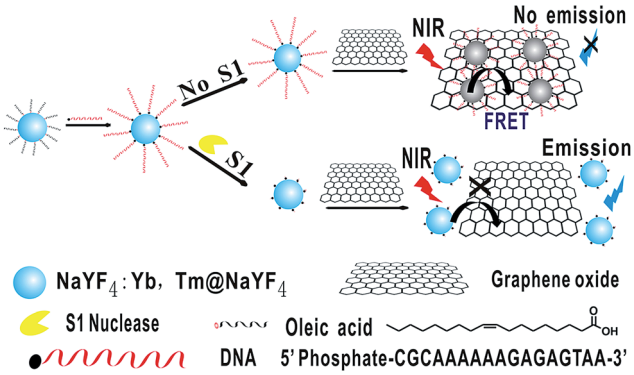

Scheme 1 Schematic illustration of the upconversion FRET-based biosensor for S1 nuclease detection.

To transfer the hydrophobic OA-coated UCNPs into the aqueous solution, the phosphate-modified DNA oligonucleotides were conjugated onto the UCNP surfaces by ligand exchange at the liquid–liquid interface. The TEM image of the resulting DNA-modified UCNPs indicated that they remained monodisperse without obvious changes in size, shape and crystallinity after modification with DNA (Fig. 1B). High-resolution TEM investigation (Fig. 1B, inset) confirmed a uniform, approximately 2 nm thick, hydrophilic DNA layer around the surface. Dynamic light scattering (DLS) measurements indicated that the DNA-modified UCNPs were well-dispersed in water, with a mean hydrodynamic diameter of about 98 nm (Fig. S1 in ESI†). In comparison with the OA-coated UCNPs dispersed in cyclohexane (*ca.* 72 nm), this increase of approximately 26 nm in diameter was in agreement with the layer of the

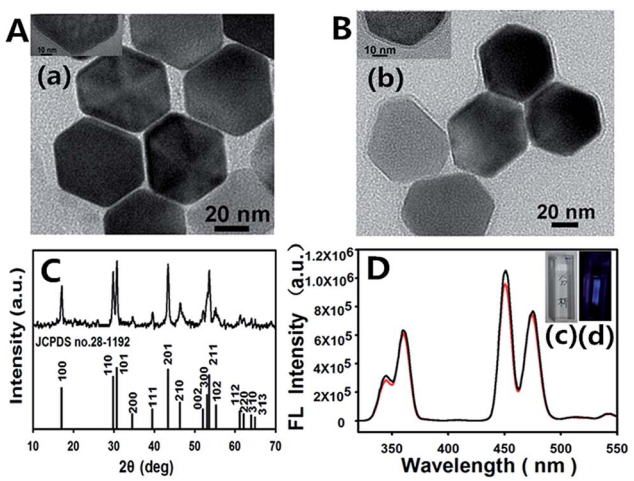

Fig. 1 TEM images of the (A) OA-UCNPs in cyclohexane and (B) DNA-modified UCNPs in water (the inset shows the high-resolution TEM images of the respective samples). (C) X-ray diffraction pattern of $NaYF_4$:Yb,Tm@$NaYF_4$ nanocrystals. (D) Upconversion fluorescence spectra of the OA-UCNPs (black curve) and DNA-UCNPs (red curve) (the inset shows a photograph of the DNA-UCNPs in water under ambient light (c) and irradiation by 980 nm light (d)).

DNA stretch in water. UV-vis absorption spectroscopy also demonstrated the conjugation of DNA oligonucleotides with the UCNPs (Fig. S2 in ESI†). The zeta potential of the resulting DNA-modified UCNPs was −9.6 mV (Fig. S3 in ESI†). In addition, the assembly of the DNA oligonucleotides on the UCNP surface was further confirmed by FT-IR (Fig. S4 in ESI†). Compared with the spectrum of the OA-coated UCNPs, new peaks at 1400 and 1082 cm^{-1} appearing in the DNA-modified UCNPs spectrum, were ascribed to the stretching vibrations of the glycosidic bond and phosphate diester bond in DNA, indicating that the DNA oligonucleotides had been successfully assembled on the UCNP surface. Furthermore, the upconversion fluorescence spectrum of the DNA-modified UCNPs in water was similar to that of the OA-coated UCNPs in cyclohexane with a slight decrease owing to the surface quenching effect of water molecules (Fig. 1D). The DNA-modified UCNPs showed excellent water solubility with long-term stability in water and resistance to aggregation over several weeks (Fig. 1D, inset). Upon continuous excitation at 980 nm, the fluorescence of the DNA-modified UCNPs in water appeared blue (Fig. 1D, inset). These results strongly indicated that the characteristic upconversion property of the nanoparticles was unaffected by the DNA coating.

3.3 Quenching effect of GO on the DNA-modified UCNPs fluorescence

The typical TEM image of the as-prepared GO (Fig. 2A) revealed that the GO sheet had occasional folds, wrinkles, and rolled edges. The strong fluorescence of the DNA-functionalizable UCNPs was sufficiently quenched (~95%) after incubation with GO (Fig. 2C), which overlapped with the absorption spectrum of GO. The TEM image shown in Fig. 2B also confirms the formation of DNA-UCNP-GO complexes. The effect of the GO concentration on the fluorescence quenching was investigated. As shown in Fig. S5 in ESI,† the upconversion fluorescence of the DNA-functionalizable UCNPs was gradually quenched with increased amounts of GO, and the quenching efficiency reached a plateau when the GO concentration was higher than 80 μg mL^{-1} (Fig. 2D). So, the GO concentration of 80 μg mL^{-1} was selected for the subsequent experiments. In addition, the incubation time of the DNA-UCNPs with GO was also studied (Fig. S6 in ESI†), and an incubation time of 60 min was used in the subsequent experiments.

3.4 Detection of S1 nuclease activity

The detection of S1 nuclease was then performed. As shown in Fig. S7 in ESI,† the incubation of S1 nuclease and the DNA-functionalized UCNPs indeed resulted in a fluorescence increase. In contrast, when Exo III and thrombin were added instead of S1 nuclease, no obvious fluorescence increases were observed under identical conditions, indicating that S1 nuclease cleaved DNA into mono- or short-oligonucleotide fragments which could decrease the adsorption of the DNA-UCNPs on the GO surface. The effect of the interaction time between the DNA-UCNPs and S1 nuclease on the fluorescence intensity was investigated, and a reaction time of 20 min was selected (Fig. S8 in ESI†). Under the optimal conditions, the upconversion fluorescence intensity increased with increasing

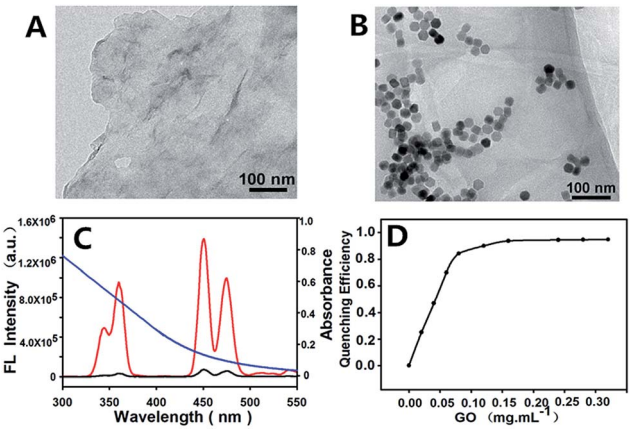

Fig. 2 TEM images of the (A) as-prepared GO and (B) DNA-functionalized UCNP-GO complexes in water. (C) Fluorescence spectra of DNA-modified UCNPs before (red curve) and after incubation with GO (black curve), and the absorption spectrum of GO (blue curve). (D) Plot of fluorescence quenching efficiency *versus* GO concentration.

S1 nuclease concentration from 1×10^{-4} to 5×10^{-2} units mL^{-1} (Fig. 3A), and the relative fluorescence intensity was linearly related to the S1 nuclease concentration (correlation coefficient $R^2 = 0.995$) in the range from 1×10^{-3} to 3×10^{-2} units mL^{-1} (Fig. 3B), and the standard deviation was obtained from three repeated experiments. Besides, it should be also noted that 1×10^{-4} units mL^{-1} S1 nuclease could be sensitively detected, with an obvious fluorescence signal. Our upconversion FRET nanosystem based method exhibited higher sensitivity in comparison to developed methods (Table S1 in ESI†). Simultaneously, compared with other types of enzymes and proteins, the proposed upconversion FRET biosensor was specific for nuclease (Fig. S9 in ESI†).

3.5 Detection of the RPMI 1640 cell medium samples

To investigate the ability of the upconversion biosensor to overcome the interference from background fluorescence and scattering light, the recovery experiment was performed in 5% (v/v) RPMI 1640 cell medium samples, the results are shown in Table 1. The recoveries were from 96% to 101% with the RSD around 6%, which are acceptable for quantitative assays performed in biological samples.

3.6 S1 nuclease activity inhibition evaluation

As an enzymatic reaction can be weakened or prohibited by its enzyme inhibitor, some enzyme inhibitors have been

Table 1 Analytical results of the S1 nuclease in RPMI 1640 cell medium samples using the upconversion biosensor

Added (units per mL)	Found (units per mL)	Recovery	RSD ($n = 3$)
1.0×10^{-3}	9.62×10^{-4}	96%	5.8%
1.0×10^{-2}	9.81×10^{-2}	98%	4.9%
2.5×10^{-2}	2.53×10^{-2}	101%	5.4%

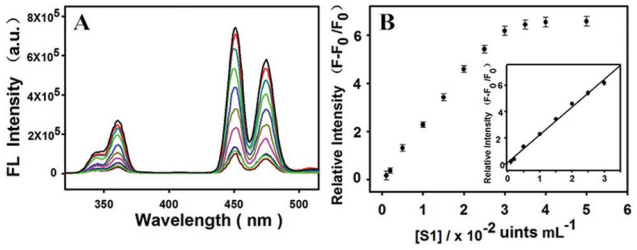

Fig. 3 (A) Upconversion fluorescence spectra of the biosensor with varying concentrations of S1 nuclease (0, 1×10^{-4}, 1×10^{-3}, 5×10^{-3}, 1.5×10^{-2}, 2×10^{-2}, 2.5×10^{-2}, 3×10^{-2} and 3.5×10^{-2} units per mL). (B) Linear relationship between the fluorescence relative intensity and the concentrations of S1 nuclease within the range of 1×10^{-3} to 3×10^{-2} units per mL. The error bars represent the standard deviations of three independent experiments.

utilized as drugs for disease therapy or as tools for adjusting the reaction rate in molecular engineering experiments. ATP, a known S1 nuclease inhibitor, was selected here to investigate its inhibition effect on the endonuclease through the proposed detection method.[26,27] As shown in Fig. S10 in ESI,† the fluorescence intensity of the upconversion FRET biosensor changes when the system adds different amounts of ATP. The results clearly showed that the activity of S1 nuclease became weaker with the increase in inhibitor concentration. The result obtained was in fair agreement with the fact that ATP has been reported to be one of the inhibitors of endonuclease S1. Therefore, our proposed method showed a great performance not only in the assay of endonuclease activity but also in the screening of endonuclease inhibitors.

4 Conclusion

In summary, we developed a facile one-step approach to make water-dispersible DNA-modified UCNPs through ligand exchange at the liquid–liquid interface, and designed a biosensor based on FRET from the DNA-functionalized UCNPs to graphene oxide. A novel ultrasensitive label-free method for assaying nuclease and activity inhibition was proposed and verified. Our upconversion FRET nanosystem based method has several advantages: first, our proposed strategy belongs to the fluorescence turn-on model, which reduces the possibility of a false positive signal and improves the detection sensitivity. In addition, the NIR-excitation technique offers non-autofluorescence assays, because of the low background signal by NIR excitation, the proposed method has a lower detection limit than UV excitation, as the fluorescence report element, the high photostability of the UCNPs can ensure ideal signal output. Furthermore, it avoids the extra step of bioconjugations using cross-linkers and directly converts the hydrophobic UCNPs into biocompatible and water-dispersible ones. Finally, our method can also be used to investigate the S1 nuclease inhibitor and employed for nuclease inhibitor screening, the assay presented here was ultrasensitive and reliable. This innovative approach provides a successful paradigm in exploring fascinating properties of upconversion FRET complexes and a new opportunity for extending their applications in a wide range of fields, such as biology, biomedicine, and more bio/chemosensing.

Acknowledgements

This work was supported by the National Natural Science Foundation of China (No. 21275045), NCET-11-0121 and the Hunan Provincial Natural Science Foundation of China (Grant 12JJ1004).

Notes and references

1 B. Y. Wu, H. F. Wang, J. T. Chen and X. P. Yan, *J. Am. Chem. Soc.*, 2011, **133**, 686–768.
2 S. J. Wu, N. Duan, X. Y. Ma, Y. Xia, Y. Yu, Z. P. Wang and H. X. Wang, *Chem. Commun.*, 2012, **48**, 4866–4868.
3 R. Gill, M. Zayats and I. Willner, *Angew. Chem., Int. Ed.*, 2008, **47**, 7602–7625.
4 M. Haase and H. Schäfer, *Angew. Chem., Int. Ed.*, 2011, **50**, 5808–5829.
5 L. N. Sun, H. S. Peng, M. I. J. Stich, D. Achatz and O. S. Wolfbeis, *Chem. Commun.*, 2009, 5000–5002.
6 H. S. Mader and O. S. Wolfbeis, *Anal. Chem.*, 2010, **82**, 5002–5004.
7 C. H. Liu, Z. Wang, H. X. Jia and Z. P. Li, *Chem. Commun.*, 2011, **47**, 4661–4663.
8 Y. H. Wang, L. Bao, Z. H. Liu and D. W. Pang, *Anal. Chem.*, 2011, **83**, 8130–8137.
9 Y. H. Wang, P. Shen, C. Y. Li, Y. Y. Wang and Z. H. Liu, *Anal. Chem.*, 2012, **84**, 1466–1473.
10 P. Zhang, S. Rogelj, K. Nguyen and D. Wheeler, *J. Am. Chem. Soc.*, 2006, **128**, 12410–12411.
11 L. Y. Wang and Y. D. Li, *Chem. Commun.*, 2006, 2557–2559.
12 F. Wang, R. R. Deng, J. Wang, Q. X. Wang, Y. Han, H. M. Zhu, X. Y. Chen and X. G. Liu, *Nat. Mater.*, 2011, **10**, 968–973.
13 F. Wang and X. G. Liu, *J. Am. Chem. Soc.*, 2008, **130**, 5642–5643.
14 H. Schäfer, P. Ptacek, K. Kömper and M. Haase, *Chem. Mater.*, 2007, **19**, 1396–1400.
15 Z. Q. Li, Y. Zhang and S. Jiang, *Adv. Mater.*, 2008, **20**, 4765–4769.
16 L. L. Li, R. B. Zhang, L. L. Yin, K. Z. Zheng, W. P. Qin, P. R. Selvin and Y. Lu, *Angew. Chem., Int. Ed.*, 2012, **51**, 1–6.
17 Y. Cen, Y. M. Wu, X. J. Kong, S. Wu, R. Q. Yu and X. Chu, *Anal. Chem.*, 2014, **86**, 7119–7127.
18 Y. M. Wu, Y. Cen, L. J. Huang, R. Q. Yu and X. Chu, *Chem. Commun.*, 2014, **50**, 4759–4762.
19 L. L. Li, P. Wu, K. Hwang and Y. Lu, *J. Am. Chem. Soc.*, 2013, **135**, 2411–2414.
20 Y. Wang, Z. H. Li, D. H. Hu, C. T. Lin, J. H. Li and Y. H. Lin, *J. Am. Chem. Soc.*, 2010, **132**, 9274–9276.
21 H. B. Wang, Q. Zhang, X. Chu, T. T. Chen, J. Ge and R. Q. Yu, *Angew. Chem., Int. Ed.*, 2011, **83**, 67276–67282.

22 N. D. F. Grindley, K. L. Whiteson and P. A. Rice, *Annu. Rev. Biochem.*, 2006, **75**, 567–605.
23 M. R. Lieber, *BioEssays*, 1997, **19**, 233–240.
24 B. Yin, J. C. Boyer, D. Habaut, N. R. Branda and Y. Zhao, *J. Am. Chem. Soc.*, 2012, **134**, 16558–16561.
25 H. Wang, Q. Zhang, X. Chu, T. Chen, J. Ge and R. Yu, *Angew. Chem., Int. Ed.*, 2011, **50**, 7065–7069.
26 P. Wrede and A. Rich, *Nucleic Acids Res.*, 1979, **7**, 1457–1467.
27 R. Cao, B. Li, Y. Zhang and Z. Zhang, *Chem. Commun.*, 2011, **47**, 12301–12303.